Ionic Changes in the Mitotic Apparatus at the Metaphase/Anaphase Transition

STEPHEN M. WOLNIAK, PETER K. HEPLER, and WILLIAM T. JACKSON*
*Department of Botany, University of Massachusetts, Amherst, Massachusetts 01003; and *Department of Biological Sciences, Dartmouth College, Hanover, New Hampshire 03755. Dr. Wolniak's present address is the Department of Botany, University of Maryland, College Park, Maryland 20742.*

ABSTRACT We have employed a series of permeant, nontoxic, fluorescent probes to detect changes in ionic conditions within the mitotic apparatus of living endosperm cells of *Haemanthus* during the transition from metaphase to anaphase. Fluorescence emission intensity measurements from the spindle for chlorotetracycline (CTC) decline before the onset of anaphase, indicating a reduction in the amount of membrane-associated Ca^{2+} and suggesting an efflux of Ca^{2+} from membrane compartments into the spindle. Subsequent to the onset of anaphase, we observe increases in fluorescence with both 8-anilino-1-naphthalene sulfonate (ANS) and 3,3′-dipentyl 2,2′-dioxacarbocyanine (diO-C_5(3)), sensitive to cationic and anionic charges at membrane surfaces, respectively. The increases with ANS and diO-C_5(3) suggest that redistributions of ions within the spindle accompany anaphase motion. During the metaphase/anaphase transition, spindle membrane content remains constant, as evidenced by unchanging fluorescence with the hydrophobic probe, N-phenyl-1-naphthylamine (NPN). Shifts in emission intensity from the nonspindle cytoplasm or from the spindle poles do not accompany the changes in fluorescence we observe in the spindle, suggesting that any ionic fluxes responsible for the changes in fluorescence are restricted to the spindle domain.

There has been considerable conjecture concerning the role of ions, especially Ca^{2+}, in the regulation of mitotic events (19, 20, 22, 24, 32). Temporally specific and spatially localized Ca^{2+} fluxes may act as "triggers" (20, 24), or as "second messengers" (7, 20, 24, 27) for the formation of the mitotic apparatus (MA) and for the initiation of anaphase chromosome motion. However, the data demonstrating Ca^{2+} levels or even static ionic conditions within the mitotic cell are meager (20, 22, 24, 36). Detection and characterization of any ionic fluxes (or associated changes in membrane potential) in the mitotic spindle could provide a basis for understanding the regulatory mechanisms involved.

A plausible time to look for changes in ion levels or in membrane potentials that may relate to a Ca^{2+} flux is at the onset of anaphase. First, the simultaneous separation at centromeres of all chromosomes (2, 28, 31) suggests, because of its coordination, the occurrence of an electrical or ionic event. Second, there is the movement of chromosomes to the poles, with the concomitant breakdown of the Ca^{2+}-sensitive spindle microtubules (13, 16, 30). It is possible that these events are Ca^{2+} triggered or regulated.

In order to detect changes in ions or associated changes in charge distribution during the metaphase/anaphase transition, we have used fluorescent membrane probes that respond to changes in ionic conditions. We have shown previously that the fluorescent-chelate probe, chlorotetracycline (CTC) (8), stains spindles of the flattened endosperm cells of *Haemanthus* and portrays the distribution of membrane-associated Ca^{2+} in living cells (45, 46). Recent reports (9, 34) indicate that decreases in CTC fluorescence accurately depict Ca^{2+} effluxes from membrane compartments both in vitro and in vivo. Ionic or potential changes that may accompany the metaphase/anaphase transition have been sought using two different charge-sensitive, permeant, nontoxic probes, 8-anilino-1-naphthalene sulfonate (ANS) (21, 43, 47, 49) and 3,3′-dipentyl 2,2′-dioxacarbocyanine (diO-C_5(3)) (4, 12, 41, 44). Our results show that CTC fluorescence declines before the metaphase/anaphase transition and that ANS and diO-C_5(3) fluorescences increase following the onset of anaphase. Membrane quantity in the spindle, as assessed by fluorescence from the hydrophobic probe N-phenyl-1-naphthylamine (NPN) (33, 38, 42), remains constant during the transition. These results suggest that changes in ion distributions accompany anaphase chromosome movement.

THE JOURNAL OF CELL BIOLOGY · VOLUME 96 MARCH 1983 598-605

MATERIALS AND METHODS

Ficoll 400, ANS, and CTC were obtained from Sigma Chemical Co. (St. Louis, MO); NPN was obtained from Eastman Kodak Co. (Rochester, NY); diO-$C_5(3)$ was kindly provided by Dr. Alan S. Waggoner (Amherst College, Amherst, MA).

Endosperm cells were expressed from immature seeds of the African Blood Lily, *Haemanthus katherinae* Baker, onto microscope slides coated with 1% Ficoll 400, as described previously (45, 46). The cell suspension was diluted by 25% through the addition of 5–20 μl of a 3.5% glucose solution containing the dissolved fluorescent probe. This addition yielded final dye concentrations as follows: CTC, 10–40 μM; NPN, 10–40 μM; ANS, 10–20 μM; diO-$C_5(3)$, 0.1–0.2 μM. None of the probes appeared to be toxic at the concentrations used. Following addition of the dye solution, the cells were covered with a Ficoll-coated coverglass (18) and incubated at room temperature for at least 20 min before observation. The coverglasses were not sealed to the slides for these experiments.

Phase contrast and fluorescence photomicrography were performed as described previously (45, 46), using a Reichert Zetopan incident-light fluorescence microscope (Reichert Optical Corp., Vienna) and Kodak Tri-X film (Eastman Kodak Co., Rochester, NY) processed with Diafine (Acufine Corp., Chicago, IL). Typical fluorescence exposures taken using the 40X, N.A. = 0.9 brightfield objective lens were 10 s or less.

Fluorescence intensity measurements were made by coupling a photomultiplier-based photometer (Custom Instruments, Albany, NY) to the Reichert microscope stand. The values of relative fluorescence emission intensity were obtained from the photometer digital display during a 5–10-s exposure of the specimen to the excitation light. The photomultiplier tube (PMT) was operated at a potential of 600 V and was filtered to integrate the signal for 10-ms intervals. Compensation for changes in dark current and/or background fluorescence was made by zeroing the photometer on a dark field of view adjacent to the cell immediately before specimen illumination. Fluctuations in photometer high voltage, in dark current or in background fluorescence, were found not to be significant. Specimen autofluorescence, assessed by monitoring changes from unstained cells, was also insignificant at the excitation intensities used. Spectral bandwidth from the 100 W, 12 VDC quartz/halogen lamp (Osram, Berlin) for CTC or diO-$C_5(3)$, or from the 200 W HBO-200 high-pressure Hg lamp (Osram, Berlin) for NPN or ANS, was controlled by selective absorption and interference filters as described in Table I. The selection of filters for excitation and emission (Table I) was dictated by the absorption and fluorescence characteristics of the probes used (Table II). Because CTC and ANS undergo spectral shifts in different apolar environments (Table II), we equipped our microscope for detection of Ca-CTC associated with membrane surfaces (8, 14, 45), and for ANS associated with membranes (21, 29). The area for emission intensity measurement was limited to a circle 12 μm in diameter by a Zeiss Aperture/Ocular (Carl Zeiss Inc., New York, NY). Using the low intensity excitation light required for cell viability (2), we determined that measurements of this area provided favorable signal-to-noise ratios, and fairly homogeneous regions in the cytoplasm of these large cells (Fig. 1). The signal-to-noise ratio obtained was at least 25 and was typically in excess of 100 (35).

Fluorescence intensity measurements were made of spindle, nonspindle, and polar regions of the cytoplasm (Fig. 1) at 2–6 min intervals in cells progressing from metaphase through early anaphase. Cells were chosen carefully to assure that the nonfluorescent chromosome arms would not enter into the 12-μm diameter field during the course of the fluorometric measurements. In spite of the long duration of anaphase in *Haemanthus* (50–90 min, depending on cell size (2)), measurements were terminated after the first 15–25 min of chromosome movement, for two reasons. First, since anaphase chromosome motion probably results in the packing of spindle constituents (i.e., binding sites for the dyes) into an increasingly smaller volume between the chromosomes and the poles, increases in fluorescence due to simple geometric changes were avoided by measuring the emission signal only during early anaphase when packing would be less significant. Second, during later stages of anaphase, the 12-μm diameter spot of measurement in the chromosome-to-pole region of the spindle would begin to exceed the distance between the leading kinetochores and the polar aggregate of mitochondria and plastids. The sudden inclusion of brightly fluorescent mitochondria and plastids in the field of measurement increases the fluorescent signal two- to five-fold over that from the spindle region alone. This nonuniformity in the 12-μm diameter field necessitated termination of the measurements during early anaphase. Data were obtained from at least seven cells for each of the probes, and for each data set the trends of changing intensities were similar. The curves presented as Figs. 6–9 are representative of the data obtained for all cells

TABLE I

Control of Spectra for Fluorometric Determinations

Probe	Excitation filters/λmax	Dichroic beam splitter	Emission filters
		nm	
CTC	BG-12/410 nm, BG-38/red supp.	490	520 nm interference* or 532 nm interference‡ (Ditric Optics, Hudson, MA)
NPN	UG-1/350 nm, BG-38/red supp.	400	UV barrier, 418 nm cutoff (Reichert Optics, Vienna)
ANS	UG-1/350 nm, BG-38/red supp.	490	515 barrier, or 520 interference (Ditric)
diO-$C_5(3)$	BG-12/410 nm, BG-38/red supp., 470 interference (Ditric)	490	510 interference (Ditric)

* Emission peak for Mg-CTC [8, 9, 10, 11].
‡ Emission peak for Ca-CTC [8, 9, 10, 11].
Control of spectra for fluorometric determinations. Excitation and emission spectra for each of the probes were limited to specific wavelength ranges in our microscope by the combinations of filters and dichroic mirrors listed. The interference fiters (Ditric Optics, Hudson, MA) had a half-brand width of 8 nm.

TABLE II

Dye Binding and Spectral Characteristics

Probe	Spectral maxima: excitation/emission	Binding site(s)	References
CTC	376 nm/520 nm	Mg-complex; polar or apolar	[8, 9, 10, 11, 14]
CTC	390 nm/530 nm	Ca-complex; apolar-membrane surfaces	[8, 9, 10, 11, 14]
NPN	350 nm/420 nm	Apolar regions-embedded in membrane lipid bilayer	[33, 42]
ANS	330–350 nm/460 nm	Apolar regions of proteins; enhanced by cations	[1, 6, 15, 21, 29, 47]
ANS	368 nm/520 nm	Apolar regions; membrane surfaces, enhanced by cations	[1, 6, 15, 21, 29, 47]
diO-$C_5(3)$	470 nm/508 nm	Membrane surfaces, enhanced by anions, also sensitive to changes in membrane potential	[4, 5, 12, 44, 48]

Absorption and emission spectra at various binding sites for CTC, NPN, ANS, and diO-$C_5(3)$. Spectral determinations have been made by other workers, primarily on in vitro systems, for each of the probes used in this study. Our choice of filters (Table I) was based on this work, to provide information from membrane surfaces.

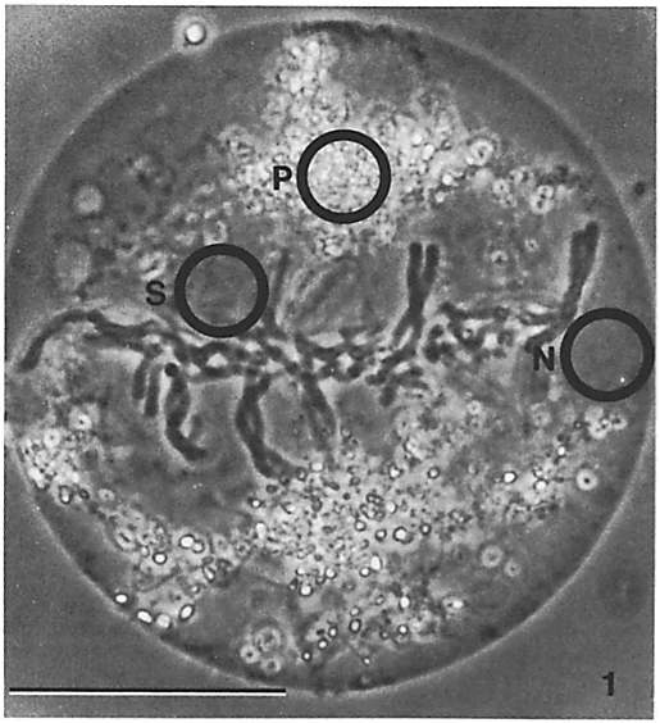

FIGURE 1 Phase contrast micrograph of an endosperm cell of *Haemanthus* at the metaphase/anaphase transition. Circles (inside diam = 12 μm) depict regions in the spindle (*S*), nonspindle (*N*), and pole (*P*) for fluorescence intensity measurements (see text). Bar, 50 μm. × 750.

treated with each of the probes. To facilitate comparison of the intensity changes, the mean of the metaphase values was calculated for each cell and was normalized to 100%. Placement of the normalized intensity curve on the independent axis (time) was made by noting carefully the occurrence of initial chromosome separation (time = 0). The extent of chromosome movement was assessed with phase contrast microscopy by measuring the distance between homologous chromosomes as anaphase progressed. Chromosome motion, as plotted in Figs. 6–9, reflects total migration of the centromeres.

RESULTS

Spindle fluorescence in *Haemanthus* endosperm at the metaphase/anaphase transition with CTC is organized in discrete, cone-shaped zones (Fig. 2*a* and *b*) that coincide with the distribution of kinetochore fiber birefringence (45). The cone-shaped zones of fluorescence (arrows, Figs. 2*b*, 4*b*, and 5*b*) are not caused by the protrusion of nonfluorescent chromosome arms into an otherwise brightly fluorescent spindle; rather, these zones represent regions of the MA that are rich in ER (25). In contrast, spindle fluorescence with the hydrophobic probe NPN (Fig. 3*a* and *b*) is less well defined, though kinetochore fiber regions exhibit greater emission intensity than do inter-fiber regions (Fig. 3*b*). NPN fluorescence (Fig. 3*b*) appears more "granular" than CTC fluorescence (Fig. 2*b*), and a portion of the NPN signal as judged visually by focusing through the cell clearly originates from the plasma membrane. Fluorescence with ANS (Fig. 4*a* and *b*) is more generally dispersed than with CTC, but less so than with NPN in the metaphase spindle; the ANS distribution is "wisp-like" and often extends across the nonfluorescent region occupied by the chromosomes (Fig. 4*b*). The fluorescence distribution with cyanine diO-C_5(3) (Fig. 5*b*) is similar to that obtained with CTC (Fig. 2*b*). Discrete cones of fluorescence appear to coincide with the birefringence of the kinetochore fibers. The intensity of the fluorescent signal with diO-C_5(3) (Fig. 5*b*) at metaphase is substantially lower than that with any of the other probes used in this study. The photographic exposure time for cells treated with diO-C_5(3) was 10–20 times longer than that for any of the other probes, under conditions of similar excitation light intensity. This difference in signal strength was also apparent from the microfluorometric measurements, below.

Serial measurements of fluorescence intensity from spindle regions of CTC-treated cells progressing from metaphase to anaphase are depicted in Fig. 6. Within 10 min of the onset of anaphase, we observe a decline in CTC emission intensity from the spindle. In the seven cells observed, the intensity from the spindle during early anaphase remained at a level lower than that detected before the initial drop late in metaphase (Fig. 6). For two of the cells, however, CTC fluorescence from the spindle increased during mid anaphase, ~11–12 min after the onset of anaphase (Fig. 6). Nonspindle fluorescence with CTC did not exhibit a reduction in intensity in late metaphase in any of the cells; similarly, CTC fluorescence from the spindle pole did not change during this period of observation.

Fluorescence in the spindle elicited by the hydrophobic probe NPN (Fig. 7) does not exhibit the marked shifts in intensity observed with CTC. Rather, NPN fluorescence during metaphase and anaphase is relatively constant, though punctuated by a transient reduction in intensity just as the chromosomes separate (Fig. 7, time = 0). There is neither a large increase nor decrease in spindle fluorescence with NPN during early anaphase, in spite of appreciable movement by the chromosomes toward the poles (Fig. 7, dotted line). The changes in spindle fluorescence are similar in the 7 cells treated with NPN.

In contrast to CTC or NPN, treatment with ANS produces very large changes in fluorescence intensity in the spindles (Fig. 8). Immediately before the initiation of chromosome separation, there is a transient reduction in ANS emission intensity and spindle fluorescence is minimal when the chromosomes separate (Fig. 8, time = 0). Subsequently, chromosome movement (Fig. 8, dotted line) is accompanied by a large increase in ANS fluorescence from the spindle (Fig. 8). Fluorescence from nonspindle cytoplasm does not increase concomitant with spindle emission (Fig. 8, curve *n* = nonspindle; *s* = spindle). In other cells treated with ANS, we find that fluorescence from the pole remains constant during the metaphase/anaphase transition. The trends in intensity changes from the spindle are identical in all nine ANS-treated cells.

As in the case of ANS, diO-C_5(3) fluorescence intensity changes in the spindle remain approximately constant during metaphase and rise sharply after the chromosomes begin to separate (Fig. 9*a* and *b*). Minimal fluorescence occurs at the onset of chromosome movement (Fig. 9*a* and *b*, time = 0). Fluorescence from the pole remains constant (Fig. 9*a*, *p* = pole) while nonspindle fluorescence levels appear to decline (Fig. 9*a*, *n* = nonspindle). As the chromosomes begin to move, spindle intensity increases (Fig. 9*a*, *s* = spindle). By mid to late anaphase, fluorescence intensity from the spindle appears to stabilize at a level higher than that during metaphase (Fig. 9*b*). The results depicted in Fig. 9*a* and *b* were obtained when the concentration of diO-C_5(3) was <0.3 μM. At higher concentrations of the probe (0.5 μM, 1.0 μM, 5.0 μM), fluorescence emission intensity during metaphase and anaphase remains constant, except for a transient decline at the onset of anaphase (time = 0), and the intensity curve from the spindle resembles that obtained with NPN (Fig. 7). The absolute intensity of cyanine fluorescence is also inversely concentration-dependent:

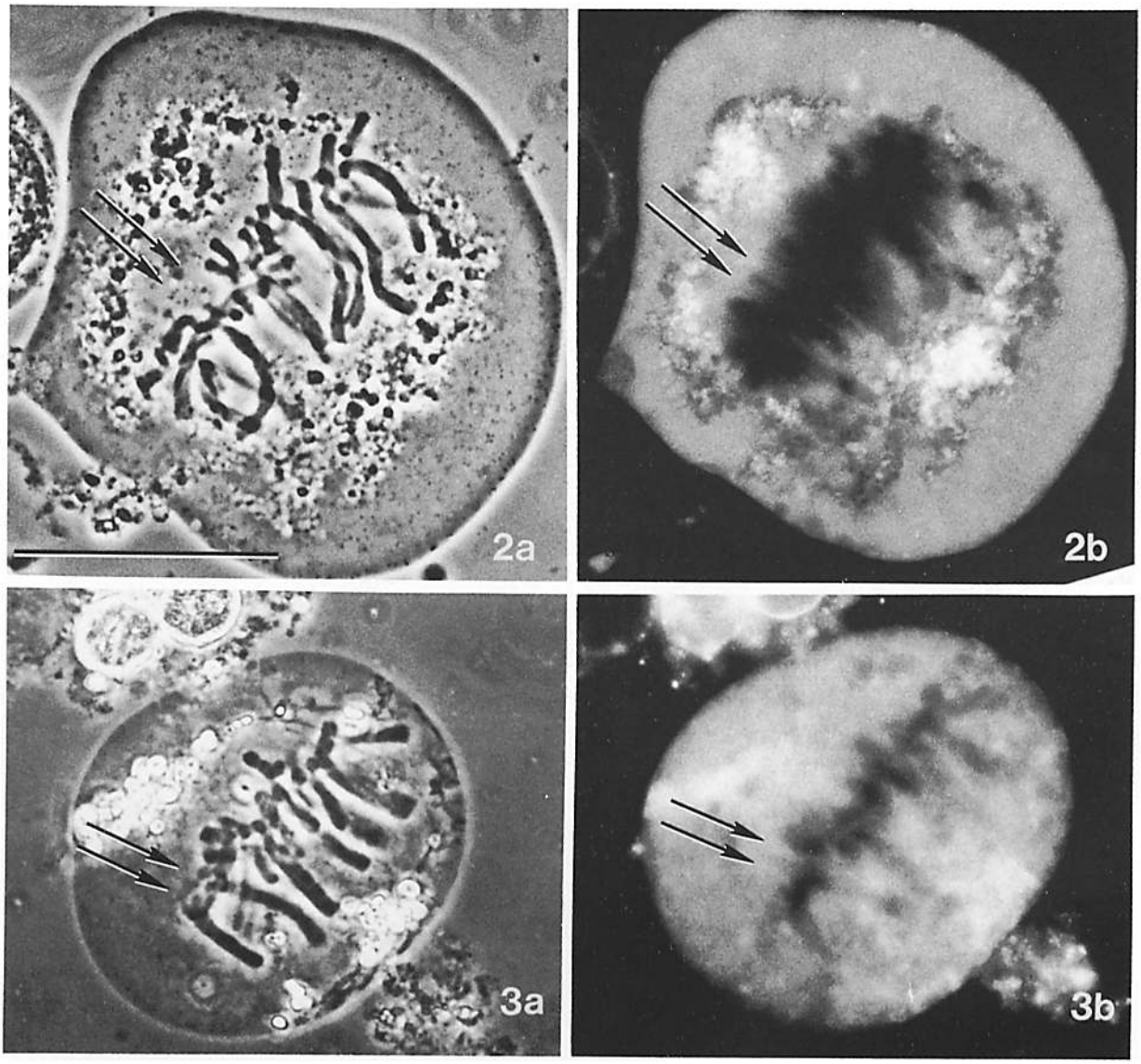

FIGURES 2 and 3 Paired phase contrast (2 *a* and 3 *a*) and fluorescence (2 *b* and 3 *b*) micrographs of *Haemanthus* endosperm cells in metaphase. Bar, 50 μm. × 750. FIGURE 2 An endosperm cell of *Haemanthus* in metaphase, pretreated for at least 20 min with 25 μM CTC. The brightest fluorescence (*b*) emanates from the polar regions of the spindle, which are rich in mitochondria and plastids (*a*). The chromosomes are dark and are surrounded by a diffuse fluorescence in the chromosome-to-pole region of the spindle. During metaphase, spindle fluorescence is actually segregated into brighter cone-shaped zones that coincide in distribution with the birefringence of the kinetochore fibers (48), and dark zones between kinetochore fiber regions. In this cell, two of these zones are indicated by the arrows. FIGURE 3 An endosperm cell of *Haemanthus* in metaphase, pretreated for at least 20 min with 25 μM NPN. As with CTC, the brightest fluorescence (*b*) originates from the polar regions of the spindle, those richest in mitochondria and plastids (*a*). The chromosomes do not fluoresce with NPN. Fluorescence in the chromosome-to-pole region of the spindle is characterized by the presence of brighter cone-shaped zones (arrows, *b*) separated by regions that are less bright but, nevertheless, fluorescent. The brighter zones coincide in distribution with the kinetochore fiber regions, but the overall appearance of spindle fluorescence is less well segregated than that observed with CTC. Fluorescence with NPN is also granular in appearance (*b*); this granularity is different from that observed with any of the other probes.

at high concentrations (>1 μM) the emission is 20–50% lower than that from dye treatments in the 0.1–0.3 μM range. The trends of change in fluorescence intensity with 0.1–0.3 μM diO-C_5(3) are similar in the three cells shown (Fig. 9 *a* and *b*) and in eight other cells observed.

DISCUSSION

Our results showing shifts of fluorescence in living mitotic cells suggest that changes in the ionic composition of the mitotic apparatus accompany or precede the onset of anaphase, and that these changes appear to be localized within the domain of the spindle. Our observed decline in CTC fluorescence (Fig. 6) is consistent with the hypothesis that a Ca^{2+} efflux from sequestered intracellular stores either "triggers" or provides the required conditions for chromosome motion (20, 24). Subsequent changes in fluorescence during early anaphase with ANS and with diO-C_5(3) further suggest that shifts in ions within the mitotic apparatus accompany the events of mitosis (24).

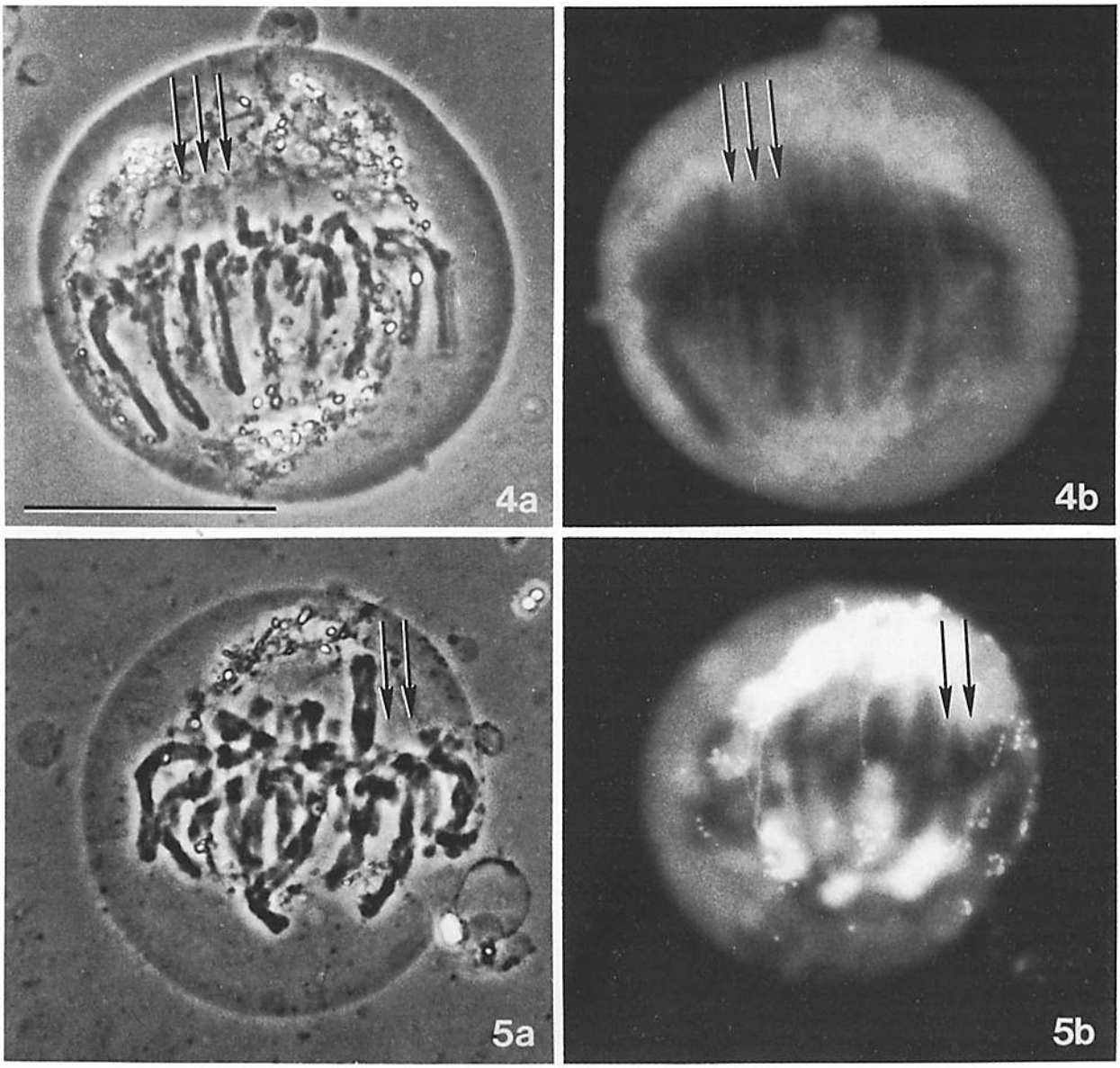

FIGURES 4 and 5 Paired phase contrast (4 *a* and 5 *a*) and fluorescence (4 *b* and 5 *b*) micrographs of *Haemanthus* endosperm cells in metaphase. Bar, 50 mm. × 750. FIGURE 4 An endosperm cell of *Haemanthus* in metaphase, pretreated at least 20 min with 15 μM ANS. The brightest fluorescence (*b*) coincides in distribution with the aggregation of mitochondria and plastids (*a*), in the polar region of the spindle. The chromosomes are dark. Fluorescence (arrows) projects toward the kinetochores from the poles and, in some instances, extends as "wispy" projections across the metaphase plate. These wisps are not apparent with CTC or NPN. FIGURE 5 An endosperm cell of *Haemanthus* in metaphase, pretreated at least 20 min with 0.2 μM diO-C_5(3). Brightest fluorescence (*b*) originates from the polar regions of the spindle, where aggregations of mitochondria and plastids are present (*a*). The chromosomes are dark. Spindle fluorescence consists of discrete cone-shaped arrays (arrows) extending from the poles toward the kinetochores; these zones are separated from each other by dark regions of the spindle, and, as is the case with all of the probes, these regions are dark even in the absence of chromosomes. The brightest lines traversing the metaphase plate (*b*) are tubular mitochondria, out of the plane of focus in the phase contrast image of the cell (*a*).

CTC and a Change in Ca^{2+} Distribution

That CTC fluorescence changes may directly follow Ca^{2+} translocations has been demonstrated in vitro by Caswell and Brandt (9). Concomitant with an induced Ca^{2+}-efflux from isolated microsomes from the sarcoplasmic reticulum, there is a decline in CTC fluorescence, which is similar to the decline we observe in the spindle before the onset of anaphase (Fig. 6). In vivo studies also demonstrate the sensitivity of CTC fluorescence to changes in the intracellular Ca^{2+} level in a variety of cell systems where declines in fluorescence accompany effluxes from membrane sequestered compartments (8, 14, 34). CTC fluorescence at 530 nm results from Ca-CTC associations at membrane surfaces (8, 10, 17); a Ca^{2+} efflux from a vesicular compartment into the cytoplasm would reduce the number of cation/membrane associations responsible for the fluorescent signal (8, 9, 10, 11). Although it has been reported that CTC responds to changes in membrane potential (12), its sensitivity is ~50 times less than that of ANS or diO-C_5(3). Moreover, the changes in CTC are separated temporally from those of ANS

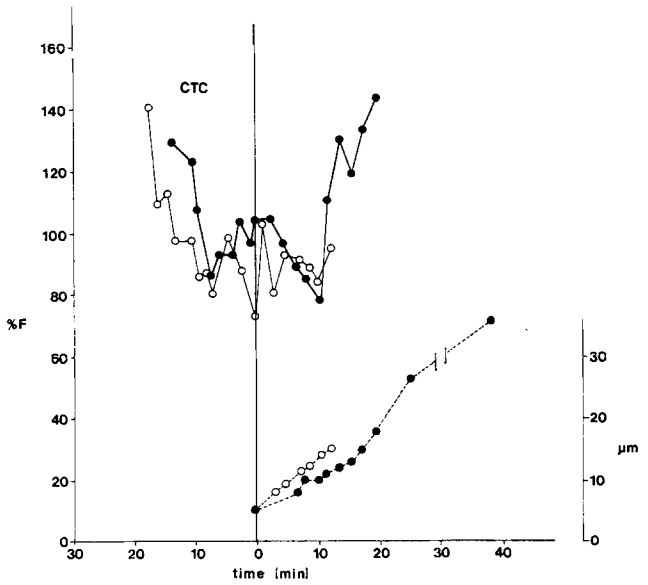

FIGURES 6–9 Fluorescence intensity changes during the metaphase/anaphase transition in living endosperm cells of *Haemanthus*. The onset of anaphase (time = 0) was judged visually by phase contrast microscopy. Values for fluorescence intensity were normalized to a percentage of the mean value obtained during metaphase (metaphase mean = 100%; see Materials and Methods).

FIGURE 6 Spindle fluorescence from two endosperm cells pretreated 20 min with 25 μM CTC during the metaphase/anaphase transition. Chromosome motion (dotted line) represents total separation of the centromeres.

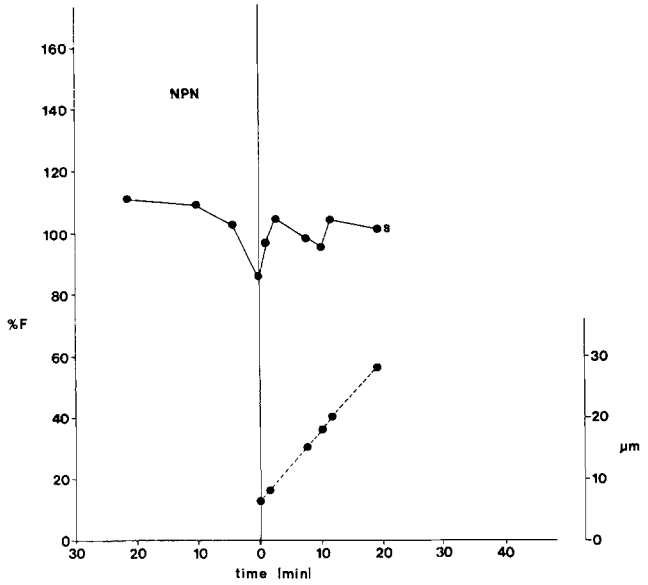

FIGURE 7 Spindle fluorescence from an endosperm cell pretreated 20 min with 25 μM NPN, during the metaphase/anaphase transition. Chromosome motion (dotted line) represents total separation of the centromeres.

and diO-C_5(3). We infer that the event reported on by CTC is electrically silent, but we cannot discount that instead it is spatially isolated from those detected by the ANS and diO-C_5(3).

In mitotic endosperm cells of *Haemanthus*, CTC fluorescence from the spindle membranes is sensitive to perturbations of intracellular Ca^{2+} (45). Thus, we suggest that the decline in CTC fluorescence from the spindle prior to the onset of anaphase (Fig. 6) represents a decline in membrane-associated Ca^{2+}. An efflux of calcium from membrane-sequestered stores is consistent with the hypothesis that a concentration increase in free Ca^{2+} in the spindle precedes and possibly triggers anaphase (19, 20, 22, 24).

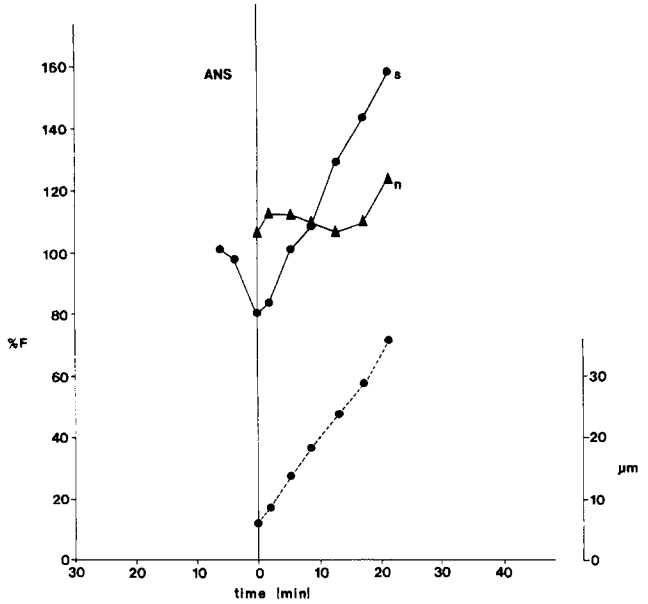

FIGURE 8 Spindle fluorescence (*s*) and nonspindle fluorescence (*n*) from an endosperm cell pretreated 20 min with 15 μM ANS. Chromosome motion (dotted line) represents total migration of the centromeres.

NPN and Spindle-Membrane Distribution

The spindle of *Haemanthus* is rich in membranes (2, 23, 25, 26), and, since anaphase fluorescence with NPN (Fig. 7) does not decline in a manner similar to that observed with CTC (Fig. 6), we infer that membrane quantity remains constant within the spindle during the metaphase/anaphase transition. NPN has been shown to map intracellular membranes by exhibiting an augmentation of fluorescence yield when embedded in a hydrophobic environment (33, 42). Because NPN fluorescence levels remain approximately constant during metaphase and early anaphase, while fluorometric measurements are made, we can discount trivial changes in spindle geometry induced by chromosome motion as an explanation for shifts in CTC, ANS, and diO-C_5(3) fluorescence. Implicit in this argument is the notion that the probes have similar affinities for cellular constituents, i.e., membranes. Though in vitro studies demonstate that hydrophobic affinities for all of these probes are high (6, 8, 12, 15, 29, 39, 41, 42, 47), and thereby suggest that membranes serve as likely locations for binding in vivo, hydrophobic zones on proteins could also function in this manner (6, 29, 39, 40, 47). The extent to which protein binding by the various dyes contributes to their fluorescence signals in vivo is not known.

The transient deflection in the NPN signal at the onset of anaphase (Fig. 7, time = 0) may result from a temporary, spatial reorganization of spindle membranes or from a change in membrane viscosity or membrane permeability (33). Although the cause of this transient is presently unknown, similar changes occur in ANS and diO-C_5(3) fluorescence at the onset of anaphase and may be due to a single common modification of membrane conformation (12, 43, 44, 47).

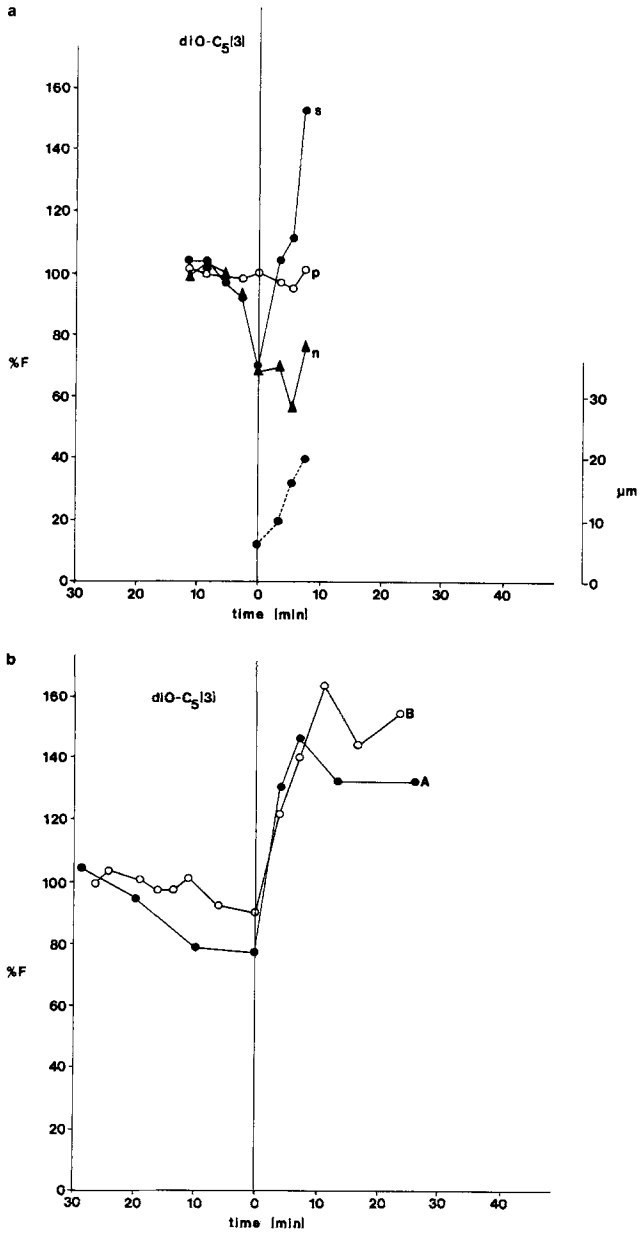

FIGURE 9 (*a*) Spindle (*s*), nonspindle (*n*), and pole (*p*) fluorescence during the metaphase/anaphase transition from an endosperm cell treated with 0.2 μM diO-C_5(3). Chromosome motion (dotted line) represents total separation of the centromeres. (*b*) Spindle fluorescence during the metaphase/anaphase transition from two endosperm cells treated with 0.2 μM diO-C_5(3).

ANS, diO-C_5(3), and Ion Redistributions

Increases in fluorescence with ANS and diO-C_5(3) at the onset of anaphase suggest that a redistribution of ions accompanies the initiation of chromosome movement. For a variety of reasons, including a lack of correlative data from conventional electro-physiology and a lack of specific knowledge about the mechanism of dye binding in dividing *Haemanthus* cells, we are not able to define the causes of the increase in ANS and diO-C_5(3) fluorescence. Nevertheless, a few conclusions can be drawn that may help us understand the events to which the dyes are responding, and that may provide clues about basic underlying ionic events of mitosis.

First, we emphasize that the fluorescence changes are spatially localized in the MA, and are temporally coupled with the onset of chromosome movement at anaphase. The organelle-rich polar regions of the spindle and the nonspindle cytoplasm do not show these changes, thus providing further support for the view that the fluorescence transients are related to specific mitosis-associated events. Second, the fluorescence signal probably emanates from the endomembranes of the MA. If the plasmalemma were responsible for the changes, then we would expect to observe them over all areas of the cell. If the membranous organelles, mitochondria and plastids, were the source of the fluctuating signal, then we would expect that the organelle-rich poles would show changes. We cannot rule out the possibility that the dyes have bound to spindle proteins (e.g., tubulin or calmodulin) and, in part, are reflecting changes therein. However, we have used filter combinations that, in vitro, enhance membrane-emitted fluorescence (Tables I, II; references 1, 14, 15, 29, 47). Third, the increases in fluorescence probably indicate an increase in dye binding. Studies on diO-C_5(3) show that an increase in fluorescence accompanies an increase in dye binding up to the point at which dye aggregation occurs. Thereafter, further accumulation of dye results in a decrease in fluorescence due to self-quenching by the dye aggregates (12, 41, 44). Our studies have been conducted with low concentrations of dye; attempts to use higher levels failed to produce fluorescence signal changes. It seems likely that at the lower levels (<0.3 μM) of dye the binding sites have not been fully saturated, and that further binding can occur which is still below the level for self-quenching aggregation. Fourth, because ANS and diO-C_5(3) are oppositely charged, and because, as argued above, both are increasing their binding to cellular sites during anaphase, we conclude that they are reporting on activities in different compartments. For example, negatively charged ANS may be responding to an increase in cations on spindle membrane surfaces (15, 21), whereas positively charged diO-C_5(3) may partition to an increasingly anionic environment (37) on the membrane facing the cisternal space. Alternatively, ANS may bind to spindle proteins such as tubulin (6) or calmodulin (29) and, in changing its fluorescence, reflect an increase in cation association.

It is evident that several schemes can be postulated to account for the fluorescence changes observed. Although both ANS and diO-C_5(3) have been utilized as "voltage-sensitive" dyes (12, 41, 43, 44, 49), it has become apparent from recent studies that membrane potential changes need not accompany large optical fluorescence changes (4, 39, 48). The possibility is raised that fluorescence changes observed with cyanine dyes, for example, may be accounted for entirely by redistributions of ions at membranous surfaces under conditions in which the membrane potential remains stationary (3, 4, 37, 48).

CONCLUSIONS

Changes in the fluorescence signals from three charge-sensitive dyes occur within the spindle region of living cells during the progression from metaphase to anaphase. Although we do not know the underlying causes for these changes, the constant signal from charge-insensitive NPN suggests that fluorescence shifts from CTC, ANS and diO-C_5(3) do not result from trivial changes in spindle geometry but, rather, describe ionic fluctuations within the spindle domain. The decline in CTC fluorescence suggests a release of Ca^{2+} from the spindle-associated membranes and is consistent with the hypothesis that a Ca^{2+} flux may trigger anaphase (20, 22, 24). The increase in ANS

and diO-$C_5(3)$ fluorescence at the onset of anaphase may also be related to changes in the free Ca^{2+} concentration, although other ions (e.g., K^+ or H^+) may be involved. These observations provide the first indications of ionic changes that are associated temporally and spatially with mitosis. Future work will focus on the molecular basis of the ionic translocations that accompany anaphase initiation.

We thank Dr. A. S. Waggoner for his helpful suggestions and for kindly providing us with the cyanine dyes used in this study. We are grateful for the comments and suggestions from Drs. P. Williamson (Amherst College), and B. Jacobson and E. Martz (University of Massachusetts). Comments from Mary Jane Saunders and Randy Wayne are also appreciated.

This work was funded by National Institutes of Health grant RO1-GM-25120 to P. K. Hepler and National Science Foundation grant PCM 80-02357 to W. T. Jackson.

Received for publication 6 May 1982, and in revised form 7 September 1982.

REFERENCES

1. Andley, U. P., and B. Chakrabarti. 1981. Interaction of 8-anilino-1-naphthalene sulfonate with rod outer segment membrane. *Biochemistry.* 20:1687–1693.
2. Bajer, A. S., and J. Molé-Bajer. 1972. Spindle dynamics and chromosome movements. *Int. Rev. Cytol.* 3(Suppl.):1–271.
3. Beeler, T. J. 1980. Ca^{2+} uptake and membrane potential in sarcoplasmic reticulum vesicles. *J. Biol. Chem.* 255:9156–9161.
4. Beeler, T. J., R. H. Farmen, and A. N. Martonosi. 1981. The mechanism of voltage-sensitive dye responses on sarcoplasmic reticulum. *J. Membr. Biol.* 62:113–137.
5. Beeler, T., J. T. Russell, and A. Martonosi. 1979. Optical probe responses on sarcoplasmic reticulum: oxacarbocyanines as probes of membrane potential. *Eur. J. Biochem.* 95:579–591.
6. Bhattacharyya, B., and J. Wolff. 1975. The interaction of 1-anilino-8-naphthalene sulfonate with tubulin: a site independent of the colchicine-binding site. *Arch. Biochem. Biophys.* 167:264–269.
7. Borle, A. B. 1981. Control, modulation and regulation of cell calcium. *Rev. Physiol. Biochem. Pharmacol.* 90:13–155.
8. Caswell, A. H. 1979. Methods of measuring intracellular calcium. *Int. Rev. Cytol.* 56:145–181.
9. Caswell, A. H., and N. R. Brandt. 1981. Ion-induced release of calcium from isolated sarcoplasmic reticulum. *J. Membr. Biol.* 58:21–33.
10. Caswell, A. H., and J. D. Hutchison. 1971. Selectivity of cation chelation to tetracyclines: evidence for special conformation of calcium chelate. *Biochem. Biophys. Res. Commun.* 43:625–630.
11. Caswell, A. H., and S. Warren. 1972. Observation of calcium uptake by isolated sarcoplasmic reticulum employing a fluorecent chelate probe. *Biochem. Biophys. Res. Commun.* 46:1757–1763.
12. Cohen, L. B., B. M. Salzberg, H. V. Davila, W. N. Ross, D. Landowne, A. S. Waggoner, and C. H. Wang. 1974. Changes in axon fluorescence during activity: molecular probes of membrane potential. *J. Membr. Biol.* 19:1–36.
13. Euteneuer, U., and J. R. McIntosh. 1980. Polarity of midbody and phragmoplast microtubules. *J. Cell Biol.* 87:509–515.
14. Fabiato, A., and F. Fabiato. 1979. Use of chlorotetracycline fluorescence to demonstrate Ca^{2+}-induced release of Ca^{2+} from the sarcoplasmic reticulum of skinned muscle cells. *Nature (Lond.).* 281:146–148.
15. Flanagan, M. T., and T. R. Hesketh. 1973. Electrostatic interactions in the binding of fluorescent probes to lipid membranes. *Biochim. Biophys. Acta.* 298:535–545.
16. Fueseler, J. W. 1975. Mitosis in *Tilia americana* endosperm. *J. Cell. Biol.* 64:159–171.
17. Hallett, M., A. S. Schneider, and E. Carbone. 1972. Tetracycline fluorescence as calcium-probe for nerve membrane with some model studies using erythrocyte ghosts. *J. Membr. Biol.* 10:31–44.
18. Hard, R., and R. D. Allen. 1977. Behaviour of kinetochore fibers in *Haemanthus katherinae* during anaphase movement of chromosomes. *J. Cell Sci.* 27:47–56.
19. Harris, P. 1975. The role of membranes in the organization of the mitotic apparatus. *Exp. Cell Res.* 94:409–425.
20. Harris, P. 1978. Triggers, trigger waves, and mitosis: a new model. *In* Monographs in Cell Biology. E. D. Buetow, I. L. Cameron, and G. M. Padilla, editors. Academic Press, New York. 25–104.
21. Haynes, D. H. 1974. 1-Anilino-8-naphthalene sulfonate: a fluorescent indicator of ion binding and electrostatic potential on the membrane surface. *J. Membr. Biol.* 17:341–366.
22. Hepler, P. K. 1977. Membranes in the spindle apparatus: their possible role in the control of microtubule assembly. *In* Mechanism and Control of Cell Division. T. Rost and E. M. Gifford, Jr. editors. Dowden, Hutchinson and Ross, Stroudsburg, PA. 212–232.
23. Hepler, P. K., and W. T. Jackson. 1968. Microtubules and early stages of cell plate formation in the endosperm of *Haemanthus katherinae* Baker. *J. Cell Biol.* 38:437–446.
24. Hepler, P. K., S. M. Wick, and S. M. Wolniak. 1981. The structure and role of membranes in the mitotic apparatus. *In* International Cell Biology, 1980–1981. H. G. Schweiger, editor. Springer-Verlag, Berlin. 673–686.
25. Jackson, W. T., and B. G. Doyle. 1982. Membrane distribution in dividing endosperm cells of *Haemanthus. J. Cell Biol.* 94:637–643.
26. Jensen, C. 1982. Dynamics of spindle microtubule organization: kinetochore fiber microtubules of plant endosperm. *J. Cell Biol.* 92:529–544.
27. Kretsinger, R. H. 1981. Mechanisms of selective signalling by calcium. *Neurosci. Res. Program. Bull.* 19:213–328.
28. Lambert, A.-M. 1980. The role of chromosomes in anaphase trigger and nuclear envelope activity in spindle formation. *Chromosoma (Berl.).* 76:295–308.
29. LaPorte, D. C., B. M. Wierman, and D. R. Storm. 1980. Calcium-induced exposure of a hydrophobic surface on calmodulin. *Biochemistry.* 19:3814–3819.
30. McIntosh, J. R., W. Z. Cande, and J. A. Snyder. 1975. Structure and physiology of the mammalian mitotic spindle. *In* Molecules and Cell Movement. S. Inoue and R. E. Stephens, editors. Raven Press, New York. 31–76.
31. Molé-Bajer, J. 1958. Cine-micrographic analysis of C-mitosis in endosperm. *Chromosoma (Berl.).* 9:322–358.
32. Moll, E., and N. Paweletz. 1980. Membranes of the mitotic apparatus of mammalian cells. *Eur. J. Cell Biol.* 21:280–287.
33. Overath, P., and H. Trauble. 1973. Phase transitions in cells, membranes, and lipids of *Escherichia coli.* Detection by fluorescent probes, light scattering and dialtometry. *Biochemistry.* 12:2625–2634.
34. Owen, N. E., and G. C. LeBreton. 1981. Ca^{2+} mobilization in blood platelets as visualized by chlorotetracycline fluorescence. *Am. J. Physiol.* 241:H613–H619.
35. Ploem, J. S. 1977. Quantitative fluorescence microscopy. *In* G. A. Meek and H. Y. Elder, editors. Analytical and Quantitative Methods in Microscopy. Cambridge University Press, Cambridge. 55–89.
36. Rink, T. J., R. Y. Tsien, and A. E. Warner. 1980. Free calcium in *Xenopus* embryos measured with ion-selective electrodes. *Nature (Lond.).* 283:658–660.
37. Russell, J. T., T. Beeler, and A. Martonosi. 1979. Optical probe responses on sarcoplasmic reticulum. Oxacarbocyanines. *J. Biol. Chem.* 254:2040–2046.
38. Saunders, M. J., and P. K. Hepler. 1981. Localization of membrane-associated calcium following cytokinin treatment in *Funaria* using chlorotetracycline. Planta 152:272–281.
39. Scordilis, S. P., H. Tedeschi, and C. Edwards. 1975. Donnan potential of rabbit skeletal muscle myofibrils. I. Electrofluorochromometric detection of potential. *Proc. Natl. Acad. Sci. USA.* 72:1325–1329.
40. Slavik, J., J. Horak, L. Rihova, and A. Kotyk. 1982. Anilinonaphthalene sulfonate fluorescence and amino acid transport in yeast. *J. Membr. Biol.* 64:175–179.
41. Sims, P. J., A. S. Waggoner, C. H. Wang, and J. F. Hoffman. 1974. Studies on the mechanism by which cyanine dyes measure membrane potential in red blood cells and phosphotidylcholine vesicles. *Biochemistry.* 13:3315–3330.
42. Trauble, H., and P. Overath. 1973. The structure of *Escherichia coli* membranes studied by fluorescence measurements of lipid phase transitions. *Biochim. Biophys. Acta.* 307:491–512.
43. Vanderkooi, J., and A. Martonosi. 1969. Sarcoplasmic reticulum. VIII. Use of 8-anilino-1-naphthalene sulfonate as a confirmational probe on biological membranes. *Arch. Biochem. Biophys.* 133:153–163.
44. Waggoner, A. S. 1979. Dye indicators of membrane potential. *Annu. Rev. Biophys. Bioeng.* 8:47–68.
45. Wolniak, S. M., P. K. Hepler, and W. T. Jackson. 1980. Detection of the membrane-calcium distribution during mitosis in *Haemanthus* endosperm with chlorotetracycline. *J. Cell Biol.* 87:23–32.
46. Wolniak, S. M., P. K. Hepler, and W. T. Jackson. 1981. The coincident distribution of calcium-rich membranes and kinetochore fibers at metaphase in living endosperm cells of *Haemanthus. Eur. J. Cell Biol.* 25:171–174.
47. Yguerabide, J., and M. C. Foster. 1981. Fluorescence spectroscopy of biological membranes. *In* Membrane Spectroscopy. E. Grell, editor. Springer-Verlag, Berlin. 199–269.
48. Zaritsky, A., M. Sihara, and R. Macnab. 1981. Measurement of membrane potential in *Bacillus subtilis*: a comparison of lipophilic cations, rubidium ion and a cyanine dye as probes. *J. Membr. Biol.* 63:215–231.
49. Zimniak, P., and E. Racker. 1978. Electrogenicity of Ca^{2+} transport catalyzed by the Ca^{2+}-ATPase from sarcoplasmic reticulum. *J. Biol. Chem.* 253:4631–4637.